

Observation of the Talbot effect for diffracted surface plasmon polaritons

D. van Oosten, M. Spasenović, and L. Kuipers

Center for Nanophotonics, FOM Institute for Atomic and Molecular Physics (AMOLF),
Science Park 113, 1098 XG Amsterdam, The Netherlands

A chain of periodically arranged subwavelength sized holes in a gold film is used to launch surface plasmon polaritons (SPPs). With a phase-sensitive near-field microscope, we visualize the diffraction pattern formed by the excited SPPs on the gold-air interface. We observe Talbot revivals close to the chain and far from the chain we observe the SPP diffraction orders. We study the behavior of both the revivals and the diffraction orders as a function of the number of holes. We find that the Talbot revivals become more pronounced as the number of holes is increased, in accordance with theory.

PACS numbers: 81.07.-b, 42.79.Dj, 68.37.Uv, 73.20.Mf, 78.66.Bz

Already in the 1830s, Talbot observed that when a grating is illuminated with a monochromatic plane wave, images of the grating can be observed at certain distances away from the grating [1]. This self-imaging effect, now commonly known as the Talbot effect, was explained much later by Lord Rayleigh [2]. Using the Fresnel diffraction integral he derived the distance z_T at which these revivals occur. In the 1950s it became clear that besides the self images observed at integer multiples of the Talbot distance z_T , images that are closely related to images of the grating can also appear at rational fractions of the Talbot distance [3, 4]. In the literature this has become known as the fractional Talbot effect. As shown by Berry and Klein, under the appropriate conditions, show fractal behavior [5]. More recently, the Talbot effect attracted the attention of the atomic physics community. It was shown that when a collimated beam of sodium atoms passes through a grating, the distribution of atoms in the beam exhibits self-images of the grating downstream [6]. This effect has been used with great success to create a matter wave interferometer that works with very large molecules [7]. In fact, the Talbot effect appears in any wave diffracted from a periodic structure, which is why we may expect it to also be important when studying the diffraction of surface plasmon polaritons [8]. Surface plasmon polaritons (SPPs) are light-like surface waves that exist on the interface between a metal and a dielectric. Besides playing a crucial role in the understanding of extraordinary transmission through metal nanohole arrays [9], SPPs are a powerful tool in the quest to build optical components at the nanoscale. A quasi-periodical arrangement of nanoholes in a metal screen can for instance be used to create a very tight focus a few micrometers away from the screen [10]. SPP waveguides have been used to produce slow SPPs [11] and to achieve strong SPP focussing [12, 13]. SPP interferometers and ring resonators [14], and diffractive elements for SPPs have all been demonstrated [15].

In this letter, we study the Talbot effect in a surface plasmon polariton field propagating on a gold-air inter-

face, as recently discussed by Dennis *et al.* [8]. We observe Talbot revivals in the SPP field launched by periodic chains of subwavelength sized holes. Furthermore, we visualize how the diffraction orders from these chains develop as the number of holes is increased. We compare our results with theory.

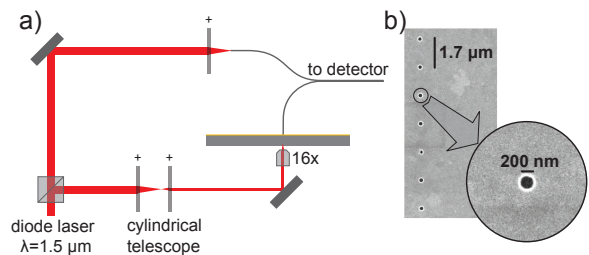


FIG. 1: (a) Schematic of the experimental setup. Light from a tunable diode laser illuminates the sample from behind. A cylindrical telescope and a 16 \times microscope objective are used to create an elliptical focal spot with a 10:1 aspect ratio. A near-field aperture probe is raster scanned over the sample, to map the electric field of the surface plasmon polaritons on the gold-air interface. The signal from the probe is interferometrically mixed with light from a reference branch. (b) Scanning electron micrograph showing a part of the sample. The diameter of the holes is 200 nm and the period of the chain of holes is 1.7 μm

Our sample consists of a BK7 glass slide on which a 200 nm thick gold film has been evaporated. In this film, chains of holes are milled using a focused ion beam (FEI Helios). A scanning electron micrograph of such a chain is shown in Fig. 1(b). We use near-field scanning optical microscopy (NSOM) to measure the SPP field. NSOM is a powerful tool to study SPPs [16] and has also been used to study waveguiding in nanoplasmonic [17] as well as nanophotonic [18] structures. Our experimental setup is illustrated in Fig. 1(a). Surface plasmon polaritons are launched onto the gold-air interface by illuminating a chain of holes with light from a diode laser source with a wavelength of 1.5 μm . With a cylindrical telescope and a microscope objective, the laser beam is focused

to an elliptical spot with beam waists in the direction perpendicular and parallel to the chain of holes of $4 \mu\text{m}$ and $40 \mu\text{m}$, respectively. A near-field aperture probe is brought in close proximity with the gold film and raster scanned over the structure. The probe has a 200 nm thick aluminum coating into which an aperture with a radius of 200 nm is opened with a focused ion beam [19]. By mixing the signal from the probe with light from a reference branch we can measure both the amplitude and phase of the electric field of the SPP [20].

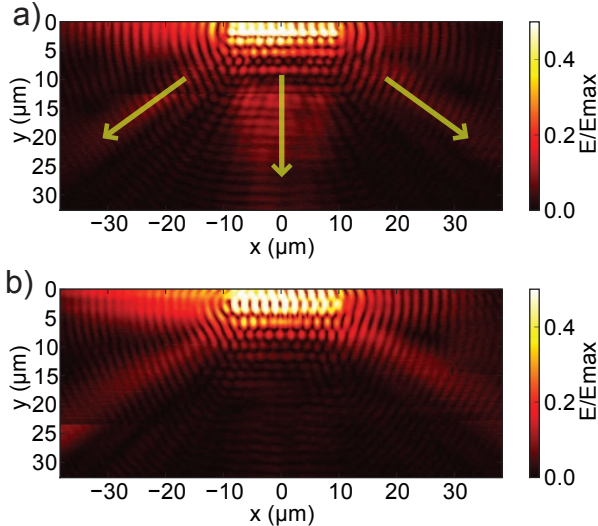


FIG. 2: Measured amplitude of the electric field of the surface plasmon polaritons (SPPs) launched by a row of 11 holes, for an incident linear polarization that is vertical (a) and horizontal (b). These data were measured with a vacuum wavelength of $1.5 \mu\text{m}$. In both images we see a strong signal directly above the holes (at the top of the images) and the weakly transmitted excitation spot (with a waist of $w_x \approx 40 \mu\text{m}$ in the horizontal direction and of $w_y \approx 4 \mu\text{m}$ in the vertical direction) around it. In the case of vertical linear polarization (a), we see a broad beam of SPPs propagating away from the chain in the positive y -direction (indicated as the 0^{th} order) and two more narrow beams of SPPs propagating away from the chain under angles of $\approx \pm 60^\circ$. In the case of horizontal linear polarization (b), the 0^{th} order is suppressed while the $\pm 1^{\text{st}}$ orders are enhanced, as expected from the SPP radiation pattern of the individual holes.

Typical results of such a measurement are shown in Fig. 2. In this measurement, a vacuum wavelength of $\lambda_0 = 1.5 \mu\text{m}$ is used. From the optical constants of gold [21], we can calculate that this corresponds to an SPP wavelength of $\lambda_{\text{SPP}} \approx 1.493 \mu\text{m}$. Note that at this wavelength, the propagation length of the SPP is more than $100 \mu\text{m}$, so we expect to see very little damping on the scale of these images. We show images, describing an area of $76 \times 32 \mu\text{m}$, of the electric field of the SPPs launched by a row of 11 holes with a spacing of $d = 1.7 \mu\text{m}$. The amplitude in the images is normalized to the maximum amplitude, which is obtained directly

above the holes in Fig. 2(a). In this image the polarization of the impinging light is chosen perpendicular to the chain of holes. We see the 0^{th} and the $\pm 1^{\text{st}}$ SPP diffraction orders (indicated by the green arrows) propagate away from the structure. The diffraction angle of the $\pm 1^{\text{st}}$ orders is found to be $\theta_{\text{out}} \approx 60^\circ$, in good correspondence with the Bragg condition $\sin \theta_{\text{out}} = m\lambda_{\text{SPP}}/d$, where d is the hole spacing and m is the diffraction order. Note that the color scale is chosen such that it saturates at a value of $E/E_{\text{max}} = 0.5$ to show the diffracted orders more clearly. When the polarization is chosen parallel to the chain (Fig. 2(b)), we clearly observe that the 0^{th} diffraction order is strongly suppressed. This suppression is caused by the fact that a circular hole does not launch SPPs in a circular pattern. Instead, due to the boundary conditions of the electric field at the edge of a hole, the SPPs are launched mainly in the direction of the impinging polarization [22, 23]. Thus, we can select the order the SPPs should diffract into by overlapping the maximum of the angular distribution of the SPPs launched by the individual holes, with the angle of that particular diffraction order.

To understand how these diffraction orders develop as a function of the number of holes in the chain, we show the phase of the SPP field launched by a chain of 3, 7, and 11 holes in Figs. 3(a), (b) and (c), respectively. The images each describe an area of $42 \times 16 \mu\text{m}$. The period of the chain is again $d = 1.7 \mu\text{m}$. We note that for 3 holes (Fig. 3(a)), the wavefronts are strongly curved in an almost circular pattern centered around the chain. In contrast, for 11 holes (Fig. 3(c)), almost plane wavefronts are observed in three directions corresponding to the 0^{th} and the $\pm 1^{\text{st}}$ SPP diffraction orders.

In Figs. 3(d-f) the amplitude of the SPP field is shown. The amplitude in these images is normalized to the maximum amplitude measured in Fig. 3(f). At the top of these images, we see chains of bright spots. These spots are as bright as they are, because light from the holes is directly picked up by the tip. At a distance of a few micrometers away from the chain, we clearly observe a modulation in the amplitude of the SPP field parallel to the chain, that has the same period as the chain of holes. These images therefore show the first observation of the Talbot effect for SPPs. In fact, the images show both integer and fractional Talbot revivals. The row of maxima closest to the chain is horizontally offset, such that the maxima are lined up between the holes. In the row of maxima below that, the maxima are aligned with the holes. This second row is the first Talbot revival. The first row is laterally shifted with respect to the holes, but has the same period. Importantly, it occurs at roughly half the distance between the chain and the first Talbot revival, which shows that this row is a fractional Talbot revival [3, 4]. Since the distance d in our measurement is on the order of the wavelength, the revivals do not occur exactly at the Talbot distance derived in the paraxial

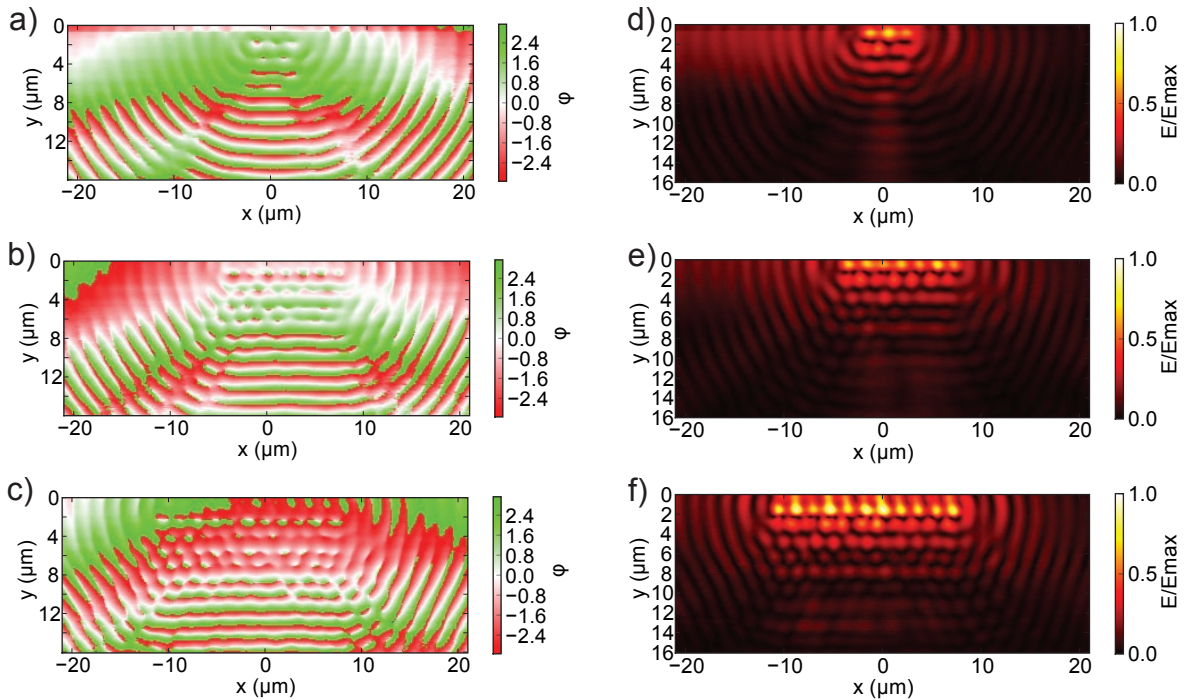


FIG. 3: Measured phase (a-c) and amplitude (d-f) of the electric field of the surface plasmon polaritons launched by rows of respectively 3 (a, d), 7 (b, e) and 11 (c, f) holes, each with a diameter of 200 nm and a spacing of 1.7 μm . All measurements were taken with a vacuum wavelength of 1.5 μm . Each image describes an area of $42 \times 16 \mu\text{m}$. The phase images (a-c) clearly show that for 3 holes the SPP field propagates almost circularly outwards from the structure, whereas for 11 holes, the SPP field develops 3 diffraction orders. The amplitude images (d-f) show that parallel to the chain of holes (the row of bright spots at the top of the images), at certain distances away from the chain, the SPP field is modulated with the same period as the chain. These are the so-called Talbot revivals. Note that as the number of holes increases, the Talbot revivals persist at larger distances away from the chain.

limit by Lord Rayleigh. When $d < 2\lambda$, it is more appropriate to calculate the Talbot distance by coherently adding up three plane waves corresponding to the SPP diffraction orders of the chain. We then find that the Talbot distance is given by $z_T = \lambda / (1 - \sqrt{1 - (\lambda/d)^2})$, which in the limit of $d \rightarrow \infty$ goes to $2d^2/\lambda$, which is exactly the Rayleigh result. We have confirmed the behavior of the Talbot revivals for $d < 2\lambda$ by comparing our analytical expression with results from a numerical calculation in which the holes are replaced by non-interacting in-plane dipole sources. In the absence of an expression for the relative amplitudes of these diffraction orders, we cannot analytically predict the modulation strength of the Talbot revivals.

When comparing the amplitude images for different numbers of holes (Figs. 3(d-f)), we see that as the number of holes increases, the Talbot revivals become more pronounced and persist to distances further away from the structure. To quantify this behavior, we determine the visibility of the Talbot revivals at different distances from the chain for various chain lengths. We define the visibility as the inner product between the amplitude along a line across the holes and the amplitude across all other horizontal lines. We normalize the visibility to the visi-

bility measured above the holes. In the regime where the hole spacing is only slightly larger than the wavelength, the fractional Talbot revivals will be shifted by half a period with respect to the full revivals, which means they will show up as having a negative visibility.

The results of the visibility analysis on both experimental data and numerically calculated SPP fields is presented in Fig. 4. The SPP fields were numerically calculated by replacing the holes by non-interacting in-plane dipole sources. We verified our analytical result, shown as vertical grey lines in Fig. 4, by first performing the analysis on a simulated SPP field corresponding to 51 holes. We have confirmed that within an area of $80 \times 20 \mu\text{m}$, the calculated pattern does not change significantly when adding more holes to the calculation, which means we can consider this simulated field to correspond to an infinitely large chain. The maxima of the visibility then indeed coincide with multiples of the Talbot length z_T . The black solid lines in Figs. 4(a), (b) and (c) correspond to numerical results for 3, 7, and 11 holes. The points in the graphs are the experimental results. As can be seen in both theory and experiment, the visibility of the revivals decays more rapidly for small numbers of holes. This can be intuitively understood, because the

distance within which the diffracted orders still mutually overlap is of the order of the length of the chain. The correspondence between theory and experiment is evident, but it is somewhat spoiled by the fact that besides the Talbot effect there is also interference between the SPP field and light directly transmitted through the gold. We also note that the experimental visibility for three holes stays roughly constant from $7\ \mu\text{m}$ onwards, at a value between 0.1 and 0.2, whereas the visibility for both 7 and 11 holes decays quickly to 0. This is caused by that fact that experimentally, strong beaming of the SPP field occurs (see Fig. 3(d)), which means that there is still a strong transverse modulation of the SPP field even at $20\ \mu\text{m}$ distance away from the structure.

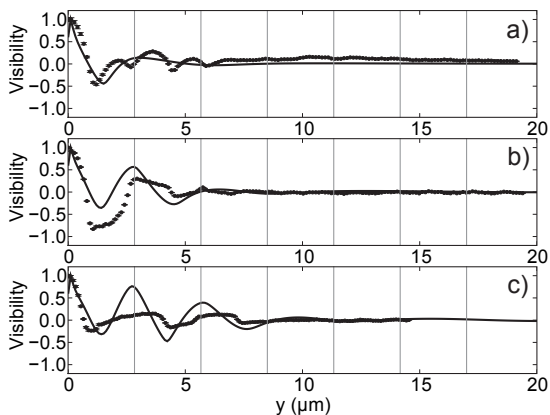


FIG. 4: The visibility of the Talbot revivals as a function of the distance away from the structure for 3 (a), 7 (b) and 11 (c) holes. As a measure for visibility, we used the inner product of a line trace taken across the holes and all other lines in the SPP field. The experimentally obtained data is represented by the dots. The solid lines are calculated from numerically simulated SPP fields. The vertical gray lines indicate where the Talbot revivals would occur for an infinitely long chain of holes.

In conclusion, we have used a chain of holes to launch surface plasmon polaritons on a gold-air interface. We have observed both the integer and the fractional Talbot effect for surface plasmon polaritons on a gold-air interface and investigated how the visibility of the Talbot revivals depends on the number of holes in the chain. We have also studied the diffraction of the surface plasmon polaritons and have shown that by changing the input polarization, we can change the direction of propagation of the surface plasmon polaritons away from the structure. These observations show that the seemingly simple structure of a chain of holes can have many exciting applications in the field of nanoplasmonics.

We thank Matteo Burrelli, Martin van Exter and Jord Prangma for fruitful discussions. The samples were fabricated at the Amsterdam nanoCenter. This work is part

of the research program of the "Stichting voor Fundamenteel Onderzoek der Materie (FOM)," which is financially supported by the "Nederlandse organisatie voor Wetenschappelijk Onderzoek (NWO)." Support by the NWO (VICI grant) is gratefully acknowledged. M. S. acknowledges the support of the EC, under the Marie Curie Scheme (contract number MEST-CT-2005-02100).

-
- [1] H. F. Talbot, *Philos. Mag.* **9**, 401 (1836)
 - [2] Lord Rayleigh, *Philos. Mag.* **11**, 196 (1881)
 - [3] E. A. Hiedemann and M. A. Breazale, *J. Opt. Soc. Am.* **49**, 372 (1959)
 - [4] J. T. Winthrop and C. R. Worthington, *J. Opt. Soc. Am.* **55**, 373 (1965)
 - [5] M. V. Berry and S. Klein, *J. Mod. Opt.* **43**, 2139 (1996)
 - [6] M. S. Chapman, C. R. Ekstrom, T. D. Hammond, J. Schmiedmayer, B. E. Tannian, S. Wehinger, and D. E. Pritchard, *Phys. Rev. A* **51**, R14 (1995)
 - [7] B. Brezger, L. Hackermüller, S. Uttenthaler, J. Petschinka, M. Arndt, and A. Zeilinger, *Phys. Rev. Lett.* **88**, 100404 (2002)
 - [8] M. R. Dennis, N. I. Zheludev, and F. J. García de Abajo, *Opt. Expr.* **15**, 9692 (2007)
 - [9] T. W. Ebbesen, H. J. Lezec, H. F. Ghaemi, T. Phio, and P. A. Wolff, *Nature* **391**, 667 (1998).
 - [10] F. M. Huang, H. I. Zheludev, Y. Chen, and F. J. García de Abajo, *Appl. Phys. Lett.* **90**, 091119 (2007)
 - [11] M. Sandtke and L. Kuipers, *Nature Phot.* **1**, 573 (2007)
 - [12] E. Verhagen, A. Polman, and L. Kuipers, *Opt. Expr.* **16**, 45 (2008)
 - [13] E. Verhagen, M. Spasenović, A. Polman, and L. Kuipers, *Phys. Rev. Lett.* **102**, 203904 (2009)
 - [14] S. I. Bozhevolnyi, V. S. Volkov, E. Devaux, J.-Y. Laluet, and T. W. Ebbesen, *Nature* **440**, 508 (2006).
 - [15] L. Feng, A. K. Tetz, B. Slutsky, V. Lomakin, and Y. Fainman, *Appl. Phys. Lett.* **91**, 081101 (2007).
 - [16] S. I. Bozhevolnyi, I. I. Smolyaninov, and A. V. Zayats, *Phys. Rev. B* **51**, 17916 (1995)
 - [17] J.-C. Weeber, J. R. Krenn, A. Dereux, B. Lamprecht, Y. Lacroute, and J. P. Goudonnet, *Phys. Rev. B* **64**, 045411 (2001)
 - [18] M. L. M. Balistreri, H. Gersen, J. P. Korterik, L. Kuipers, and N. F. van Hulst, *Science* **294**, 1080 (2001)
 - [19] J. A. Veerman, A. M. Otter, L. Kuipers, and N. F. van Hulst, *Appl. Phys. Lett.* **72**, 3115 (1998)
 - [20] M. Sandtke, R. J. P. Engelen, H. Schoenmaker, I. Attema, H. Dekker, I. Cerjak, J. P. Korterik, F. B. Segerink, and L. Kuipers, *Rev. Sci. Instrum.* **79**, 013704 (2008)
 - [21] P. B. Johnson and R. W. Christy, *Phys. Rev. B* **6**, 4370 (1972)
 - [22] C. Sönnichsen, A. C. Duch, G. Steiniger, M. Koch, G. von Plessen, and J. Feldmann, *Appl. Phys. Lett.* **76**, 140 (2000)
 - [23] L. Yin, V. K. Vlasko-Vlasov, A. Rydh, J. Pearson, U. Welp, S.-H. Chang, S. K. Gray, G. C. Schatz, D. B. Brown, and C. W. Kimball, *Appl. Phys. Lett.* **85**, 467 (2004)